

Analysis on Addition of Novel Sm^{3+} in Replacing Eu^{3+} in $\text{LiEu}_{(0.45-x)}\text{Gd}_{0.55}(\text{MoO}_4)_2$ Phosphor

M. FATHULLAH^{a,b,*}, R. HUSSIN^c, Z. SHAYFULL^{a,b},
M.M.A. ABDULLAH^a AND N.S. ZAILANI^b

^aCenter of Excellence Geopolymer & Green Technology (CEGeoGTech),
Universiti Malaysia Perlis (UniMAP), 01000 Kangar, Perlis, Malaysia

^bSchool of Manufacturing Engineering, Universiti Malaysia Perlis (UniMAP),
Pauh Putra Campus, 02600 Arau, Perlis Malaysia

^cDepartment of Physics, Faculty of Science, Universiti Teknologi Malaysia,
Skudai, Johor, Malaysia

Doi: [10.12693/APhysPolA.138.257](https://doi.org/10.12693/APhysPolA.138.257)

*e-mail: fathullah@unimap.edu.my

Europium is amongst the most critical and expensive rare earths due to its luminescence properties for red element in displays and lighting technology. As the market demand of Europium is now at scarce, this paper tried minimize the use of Europium. In the mean time, Samarium (Sm^{3+}) has been of interests as it can contribute in the red/orange emitting activator but researches of Sm^{3+} potentials in replacing Eu^{3+} was hardly found. In this article, a series of red phosphors $\text{LiEu}_{(0.55-x)}\text{Gd}_{0.45}(\text{MoO}_4)_2\text{Sm}_x$ were synthesised using solid-state reaction and an XRD analysis conducted confirmed that the structure of the compounds to remain as tetragonal scheelite structure. Results showed that 0.10 mol of Sm^{3+} can increase the luminescence intensity and the overlaid patterns show that there are no additional peaks occurred in the increasing of Sm^{3+} to the compound which confirm that the structure remained tetragonal scheelite structure with space group $I4_1/a$. This finding has opened an opportunity for industries and researchers to use Sm^{3+} in reducing the cost of consuming Eu^{3+} in lighting technologies.

topics: $\text{LiEu}(\text{MoO}_4)_2$, crystal structure, red phosphor, samarium, Molybdate

1. Introduction

On-going developments of white light emitting diodes (WLEDs) has led to a renewed interest Europium (III) Eu^{3+} . The Eu^{3+} has been used for its interesting red element in the LEDs as it emits at ~ 615 nm due to ${}^5\text{D}_0 \rightarrow {}^7\text{F}_2$ transition, and excited at 395 nm and 465 nm [1–2]. In protecting the human visual system, various types of coatings blocking UV radiation are used [3, 4]. A number of researchers reported that phosphor-based lightings has high absorption in the near-UV regions, but is chemically instable to environment. However, this aspect does not occur to molybdate based phosphor. Recently, there is an increasing interest on molybdate based phosphoras host materials in producing red based emitting source [5–10]. This material was reported to have excellent thermal and chemical stabilities with broad absorption bands near-UV regions, referring to the charge transfer from oxygen to the active centers of Eu^{3+} [2, 5–7, 9, 11–13]. In our previous report [8], $\text{LiEu}_{(1-x)}\text{Gd}_x(\text{MoO}_4)_2$ ($x = 0$ to 1) was synthesized using solid state reaction method. One of the conclusion was that the optimum amount of Eu^{3+} concentration that can be employed in the lattice was 0.45 mol with

the luminous efficacy 143.77 lm/W at excitation 395 nm and 200.57 lm/W at excitation 465 nm. Therefore, this finding opens a new initiative of developing more efficient red phosphor. In this work, a maximum of 45% of Eu^{3+} will be introduced with Samarium (III) Sm^{3+} with general equation for the experiment $\text{LiEu}_{(0.45-x)}\text{Gd}_{0.55}(\text{MoO}_4)_2\text{Sm}_x$ where $x = 0$ –0.45. The crystal structure, morphology and the photoluminescence properties of the phosphor were analysed.

2. Experimental

$\text{LiEu}_{(0.45-x)}\text{Gd}_{0.55}(\text{MoO}_4)_2\text{Sm}_x$ was synthesized using solid-state reaction where $x = 0, 0.05, 0.10, 0.15, 0.20, 0.25, 0.30, 0.35, 0.40$ and 0.45 mol. The starting materials used are Lithium carbonate 99.9%, gadolinium oxide 99.99%, molybdenum oxide (VI) $\geq 99.5\%$, europium oxide (Eu_2O_3), and samarium oxide (Sm_2O_3). The stoichiometric amount of the reactants were mixed and then calcined for 3 h at 850° in open air. Finally, the compounds were cooled at room temperature and gently ground to remove the sample powder from the crucible. The structural characterization of the red phosphors are conducted by X-ray

TABLE I

Lattice parameters and cell volumes of $\text{LiEu}_{(0.45-x)}\text{Gd}_{0.55}(\text{MoO}_4)_2\text{Sm}_x$.

Eu ³⁺	Sm ³⁺	A [Å]	C [Å]	Vol. [Å ³]	R _{wp}
0.45	0	5.196314 (68)	11.32450 (18)	305.7805 (94)	10.74
0.40	0.05	5.196648 (86)	11.32445 (23)	305.819 (12)	11.18
0.20	0.25	5.198871 (86)	11.33001 (24)	306.230 (12)	10.79
0	0.45	5.20268 (14)	11.34281 (39)	307.026 (20)	14.49

Powder Diffraction (XRPD), Bruker D2 Phaser with CuK_α radiation ($\lambda = 1.54184 \text{ \AA}$) in the range of $2\theta = 10^\circ\text{--}90^\circ$. This characterization is important because it allows to identify changes to crystal structure [14]. The morphology of the samples were observed using Hitachi TM3000 scanning electron microscope (SEM). Photoluminescence properties were measured from Perkin Elmer, LS 55 spectrometer. All the emission intensity were collected at room temperature.

3. Results and discussions

The X-ray powder diffraction (XRPD) patterns of $\text{LiEu}_{(0.45-x)}\text{Gd}_{0.55}(\text{MoO}_4)_2\text{Sm}_x$, where $x = 0, 0.05, 0.25$, and 0.45 are plotted in Fig. 1. The samples were observed to fit appropriately with the standard PDF 01-080-7695 as reference model. The overlaid patterns show that there are no additional peaks occurred in the increasing of Sm^{3+} to the compound confirming that the structure remained tetragonal scheelite structure with space group $I4_1/a$. These findings also prove that the phosphors did not undergo any phase transformation and Sm^{3+} has successfully substituted into the host phosphor.

The samples were then refined using TOPAS software using $\text{LiEu}(\text{WO}_4)_2$ as the reference model for fitting. The refinement analysis data shows that the sample of $\text{LiEu}_{(0.45-x)}\text{Gd}_{0.55}(\text{MoO}_4)_2\text{Sm}_x$ closely fits to the reference model since the value of R_{wp} are found to be a small value. The lattice's volume calculated for $\text{LiEu}_{(0.45-x)}\text{Gd}_{0.55}(\text{MoO}_4)_2\text{Sm}_x$ are shown in Table I. One can indicate the best value of $R_{wp} = 10.74$, and also the change of lattice's volume from 305.7805 \AA^3 to 307.026 \AA^3 , as the Sm^{3+} increases in the host lattice. This is due to the ionic radius of Sm^{3+} (1.079) is larger than the ionic radius of Eu^{3+} (1.066) (with eight coordination number).

Figure 2 shows the refined crystal structures of $\text{Gd}_{0.55}(\text{MoO}_4)_2\text{Sm}_{0.45}$ which is tetragonal scheelite structure with space group $I4_1/a$. One can noticed that each Mo^{6+} is surrounded with four oxygen making the tetrahedral shape in the lattice which is in line with previous findings [6–8]. Since the structures can be seen remained as Sm^{3+} increases in the host compound, it therefore indicates that the structure remains as a tetragonal scheelite structure. Figure 3 shows the morphologies with 2k magnification of the $\text{LiEu}_{(0.45-x)}\text{Gd}_{0.55}(\text{MoO}_4)_2\text{Sm}_x$

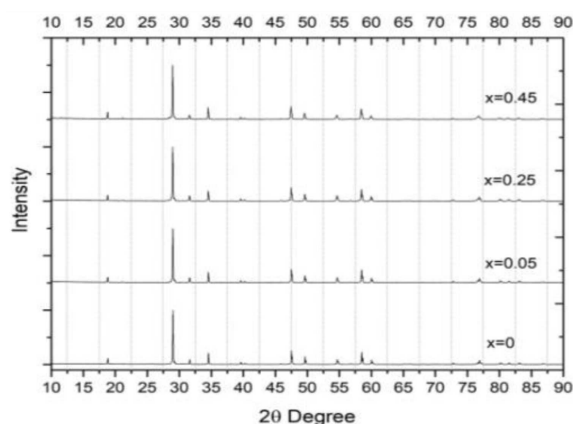


Fig. 1. The XRPD stack patterns of $\text{LiEu}_{(0.45-x)}\text{Gd}_{0.55}(\text{MoO}_4)_2\text{Sm}_x$, where $x = 0, 0.05, 0.25$ and 0.45 .

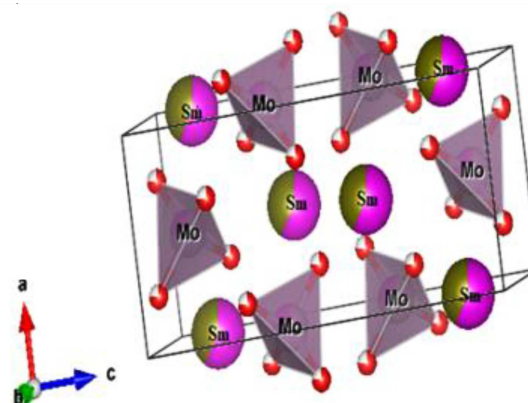


Fig. 2. Modelled crystal structure of compound $\text{LiGd}_{0.55}(\text{MoO}_4)_2\text{Sm}_{0.45}$.

($x = 0, 0.05$ and 0.45). The SEM images show that the particle of the compound is sized ranging between $1\text{--}6 \mu\text{m}$. It also can be seen that the particle shape remains the same with the additional Sm^{3+} to the host compound. In this way, the strong adherence can be seen on the phosphor $\text{LiEu}_{0.40}\text{Gd}_{0.55}(\text{MoO}_4)_2\text{Sm}_{0.05}$ (in Fig. 3a) and $\text{LiGd}_{0.55}(\text{MoO}_4)_2\text{Sm}_{0.45}$ (in Fig. 3b). In fact, the $\text{LiEu}_{0.45}\text{Gd}_{0.55}(\text{MoO}_4)_2$ compound has less adherence compared to both mentioned compounds.

The $\text{LiEu}_{(0.45-x)}\text{Gd}_{0.55}(\text{MoO}_4)_2\text{Sm}_x$ emission spectra is shown in Fig. 4, and it ranges from $550\text{--}750 \text{ nm}$ as Sm^{3+} increases from 0 to 0.45 . The highest emission intensity is seen at 615 nm due to the ${}^5\text{D}_0 \rightarrow {}^7\text{F}_2$ transition which is in line with

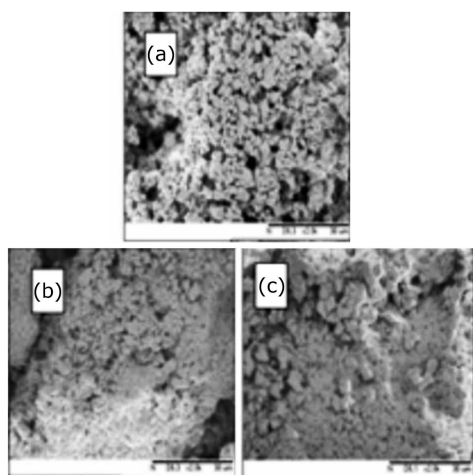


Fig. 3. Morphologies pictures obtained for the samples: (a) $\text{LiEu}_{0.45}\text{Gd}_{0.55}(\text{MoO}_4)_2$, (b) $\text{LiEu}_{0.40}\text{Gd}_{0.55}(\text{MoO}_4)_2\text{Sm}_{0.05}$, and (c) $\text{LiGd}_{0.55}(\text{MoO}_4)_2\text{Sm}_{0.45}$.

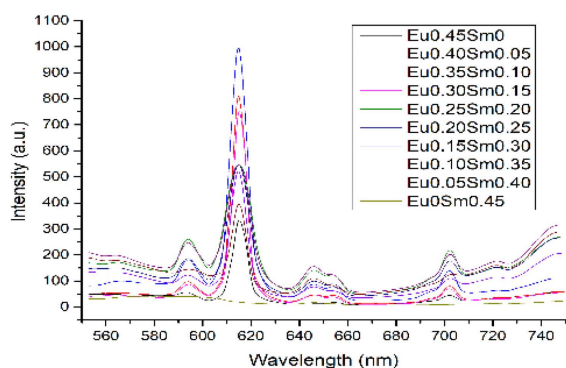


Fig. 4. Emission spectra of the red phosphor $\text{LiEu}_{(0.45-x)}\text{Gd}_{0.55}(\text{MoO}_4)_2\text{Sm}_x$ (where $x = 0$ until 0.45) obtained in the range 550 nm–750 nm.

the previous reports [5, 6, 15–17]. Another emission peaks are observed at 588–600 nm ($^5\text{D}_0 \rightarrow ^7\text{F}_1$ transition), 650–660 nm ($^5\text{D}_0 \rightarrow ^7\text{F}_3$ transition) and 690–710 nm ($^5\text{D}_0 \rightarrow ^7\text{F}_4$ transition).

As shown in Fig. 5, the emission intensity increases and approaches the maximum intensity at 0.10 mol Sm^{3+} concentration, and then gradually drops remaining constant at 0.20 mol Sm^{3+} . However, the lowest intensity has been collected since the concentration Sm^{3+} at 0.45 mol which means that the Sm^{3+} has taking all the emission of Eu^{3+} in the compound.

Figure 6 shows the normalized graph of the $\text{LiEu}_{(0.45-x)}\text{Gd}_{0.55}(\text{MoO}_4)_2\text{Sm}_x$ phosphor. It clearly shows that there are the broadening effects that occur when Sm^{3+} increases.

These quenching effects prove that the Sm^{3+} ions has taking place of the emission of Eu^{3+} ions in the host compound. With the best intensity, the concentration of Eu^{3+} can be reduced up to 0.35 mol. This is connected to the fact that the

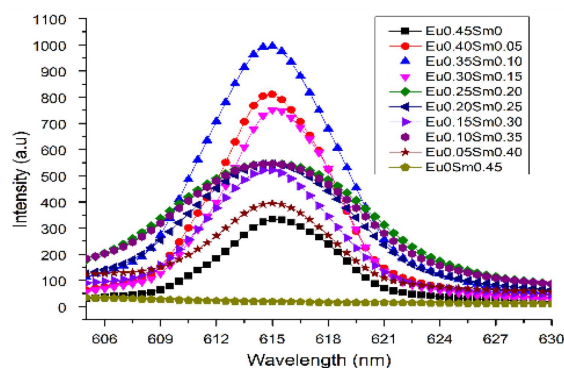


Fig. 5. Emission spectra of the red phosphor $\text{LiEu}_{(0.45-x)}\text{Gd}_{0.55}(\text{MoO}_4)_2\text{Sm}_x$ ($x = 0$ until 0.45) obtained in the range 605 nm–630 nm.

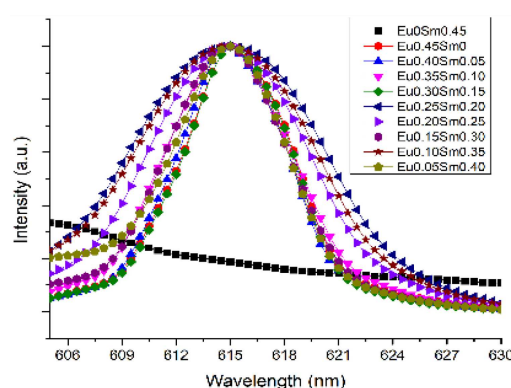


Fig. 6. Normalized graph of emission spectra of the $\text{LiEu}_{(0.45-x)}\text{Gd}_{0.55}(\text{MoO}_4)_2\text{Sm}_x$ ($x = 0$ until 0.45) in the range 605 nm–630 nm.

gap between Eu^{3+} - Eu^{3+} becomes ideal when enhanced until 0.35 mol of Eu^{3+} . However, when the gap Eu^{3+} - Eu^{3+} becomes further and further enhanced, the concentration is gradually dropped due to the absence of more Eu^{3+} .

4. Conclusion

In summary, a series of red emitting phosphor $\text{LiEu}_{(0.45-x)}\text{Gd}_{0.55}(\text{MoO}_4)_2\text{Sm}_x$ ($x = 0, 0.05, 0.10, 0.15, 0.20, 0.25, 0.30, 0.35, 0.40$, and 0.45) was successfully synthesized using solid state reaction. The XRPD results indicate that by introduced Sm^{3+} to the host lattice has no effect to the crystal structure and remains as tetragonal scheelite structure with space group $I4_1/a$. The angular shaped with particle sizes ranging between 1–6 μm were observed for the morphology analysis. The highest emission intensity located at 615 nm corresponding to $^5\text{D}_0 \rightarrow ^7\text{F}_2$ transition. The optimum amount of Sm^{3+} concentration that can be employed in the $\text{LiEu}_{(0.45-x)}\text{Gd}_{0.55}(\text{MoO}_4)_2\text{Sm}_x$ is 0.10 mol. Hence, the current red phosphor $\text{LiEu}_{0.35}\text{Gd}_{0.55}(\text{MoO}_4)_2\text{Sm}_{0.10}$ has great potential to be used as a red phosphor for near-UV-LED.

Acknowledgments

We would like to acknowledge and thank you for funding and support from the Ministry of Higher Education Malaysia MOHE through the Fundamental Research Grant Scheme (FRGS), i.e., FRGS/1/2016/STG07/UNIMAP/02/1, Application ID 218885-247922 and code 9003-00572.

References

- [1] S. Hwang, B.-A. Kang, S. Hwangbo, Y.-S. Kim, J.-T. Kim, *Electron. Mater. Lett.* **6**, 27 (2010).
- [2] J. Ru, S. Ying, W. Zheng, J. Chen, *Mater. Res. Bull.*, **84**, 468 (2016).
- [3] M. Gacek, J. Wysocki, J. Gondro, F. Badura, S. Letkiewicz, *Mater. Plast.* **56** (3), 621 (2019).
- [4] K. Jez, M. Nabialek, K. Gruszka, M. Deka, S. Letkiewicz, B. Jez, *Mater. Plast.* **55** (3), 438 (2018).
- [5] L. Ying, Y. Wang, L. Wang, Y.Y. Gu, S. Yu, Z.G Lu, R. Sun, *RSC Adv.* **4**, 4754 (2014).
- [6] M. Fathullah, *Ph.D. Thesis*, Brunel University, London 2016.
- [7] Q.F. Wang, L. Ying, W. Yu, W. Wenxi, W. Yi, W. Gui-Gen, L. Zhou-Guang, *J. Alloys Compd.* **625**, 355 (2015).
- [8] C.H. Chiu, M. F. Wang, C.S. Lee, T.M. Chen, *J. Solid State Chem.* **180**, 619 (2007).
- [9] L. Zhou, W. Wang, S. Yu, B. Nan, Y. Zhu, Y. Shi, S. Haohong, Z. Xingzhong, L. Zhouguang, *Mater. Res. Bull.* **84**, 429 (2016).
- [10] D. Zhao, J.-C. Shi, C.-K. Nie, R.-J. Zhang, *Optik*, **138**, 476 (2017).
- [11] C. Guo, S. Wang, T. Chen, L. Luan, Y. Xu, *Appl. Phys. A* **94**, 365 (2009).
- [12] K.N. Shinde, S.J. Dhoble, A. Kumar, *J. Rare Earths* **29**, 527 (2011).
- [13] N. Verma, K.C. Singh, B. Marí, M. Mollar, J. Jindal, *Acta Phys. Pol. A* **132**, 1261 (2017).
- [14] V. Đorđević, Ž. Antić, M.G. Nikolić, M.D. Damićanin, *J. Res. Phys.* **37**, 47 (2013).
- [15] L. Yi, X. He, L. Zhou, F. Gong, R. Wang, J. Sun, *J. Lumin.* **130**, 1113 (2010).
- [16] C. Guo, F. Gao, L. Liang, B.C. Choi, J.H. Jeong, *J. Alloys Compd.* **479**, 607 (2009).
- [17] A. Xie, X. Yuan, F. Wang, *Sci. China Technol. Sci.* **54**, 70 (2011).